

**This is the preprint version of the contribution published as:**

Wang, C., Wania, F., **Goss, K.-U.** (2018):

Is secondary organic aerosol yield governed by kinetic factors rather than equilibrium partitioning?

*Environ. Sci.-Proc. Imp.* **20** (1), 245 - 252

**The publisher's version is available at:**

<http://dx.doi.org/10.1039/c7em00451f>

# 1 **Is Secondary Organic Aerosol Yield Governed by Kinetic** 2 **Factors Rather Than Equilibrium Partitioning?**

3 Chen Wang<sup>1</sup>, Frank Wania<sup>1</sup>, and Kai Uwe Goss<sup>2,3\*</sup>

4 <sup>1</sup>*Department of Physical and Environmental Sciences and Department of Chemistry, University*  
5 *of Toronto Scarborough, 1265 Military Trail, Toronto, ON, M1C 1A4, Canada*

6 <sup>2</sup>*Department of Analytical Environmental Chemistry, Centre for Environmental Research UFZ*  
7 *Leipzig-Halle, Permoserstraße 15, Leipzig, D-04318, Germany*

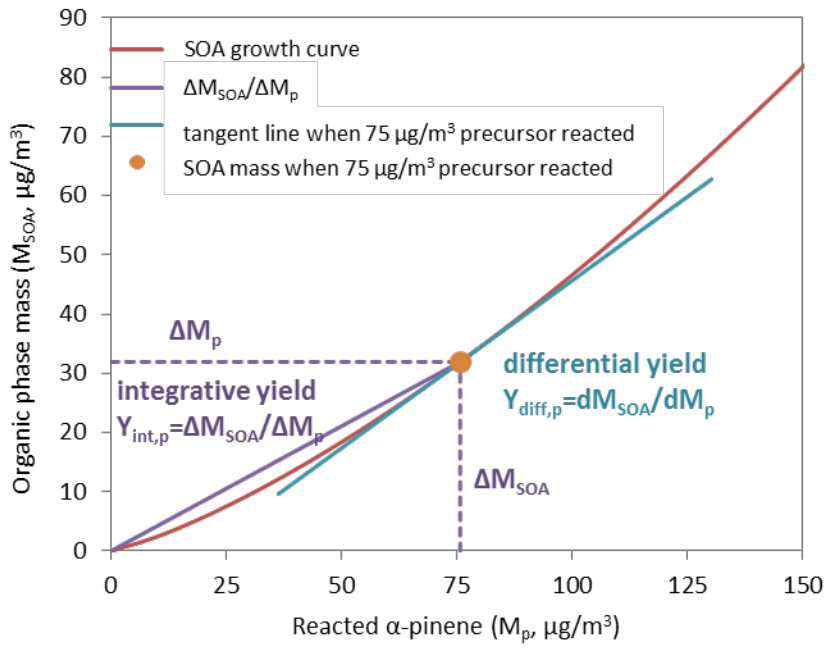
8 <sup>3</sup>*Institute of Chemistry, University of Halle-Wittenberg, Kurt-Mothes-Straße 2, Halle, D-06120,*  
9 *Germany*

10 *\*Corresponding author: kai-uwe.goss@ufz.de, ++49 341 235 1411*

## 11 **Environmental Significance**

12 Secondary organic aerosol (SOA) comprises a major fraction of atmospheric fine particles.  
13 Predicting the formation of SOA in atmospheric models is essential for evaluating their  
14 influence on climate and human health. SOA yield as an important parameter describing the  
15 efficiency of a precursor in generating aerosol materials in chamber studies, has been proposed  
16 and used for decades, despite its limitations when applied to the ambient atmosphere. A  
17 complex and dynamic system, the atmosphere's (gas and particle) composition is a result of  
18 competing kinetics of continuous emissions as well as chemical and physical processing. In this  
19 work, we emphasize the significance of the dynamic nature of the atmosphere and suggest the  
20 use of the differential SOA yield when describing SOA formation in realistic scenarios. We  
21 demonstrate the importance of the differential SOA yield with a model approach using the  $\alpha$ -  
22 pinene SOA system as an example.

23 **Graphical Abstract**



24

25 **Abstract**

26 The numerical description of the formation of secondary organic aerosol (SOA) in the  
27 atmosphere relies on the use of particle yields, which are often determined in chamber  
28 experiments. What is sometimes not appreciated is that such yields (i) can be defined in  
29 different ways and (ii) depend on atmospheric conditions. Here we show with the help of  
30 hypothetical scenario simulations that the differential SOA yield upon addition of oxidation  
31 products to an atmosphere already containing such products and SOA is more relevant in the  
32 ambient atmosphere than the commonly used integrative yield from chamber studies.  
33 Furthermore, we suggest that the SOA formation scenarios that have been studied so far  
34 comprise merely a subset of possible atmospheric situations. In particular, while in the standard  
35 scenarios factors such as volatility and aerosol loading are important, scenarios can be  
36 envisaged where these factors become less important while the differential yield approaches  
37 unity for all oxidation products. Finally, we suggest aerosol growth in the atmosphere should be  
38 seen as being determined by a dynamic situation arising from many simultaneously occurring  
39 kinetic processes rather than a thermodynamic equilibrium process.

## 40 1. Introduction

41 As a major component of atmospheric fine particles, secondary organic aerosol (SOA) plays a  
42 significant role in atmospheric processes relevant to climate and human health. <sup>1</sup> One of the  
43 primary goals of SOA research is the prediction of the quantity of SOA being formed, which is a  
44 major challenge because of the complex composition and constant transformation of  
45 compounds in the atmosphere. <sup>2</sup> The concept of particle yield is central in this effort. Studying  
46 simplified systems using both experimental and computational methods contributes to our  
47 understanding of the amount and composition of SOA formed in the atmosphere. <sup>3</sup>

48 Laboratory studies relying on smog chambers often examine SOA formation and aging  
49 processes of individual precursors to understand their relative contributions in regional and  
50 global SOA budgets. They can be conducted in batch or continuous flow mode. <sup>4</sup> Precursor  
51 compounds are introduced into a chamber and oxidized at specific conditions (temperature, RH,  
52 oxidants, light, seed particles, etc.). At the end of the experiment (usually when the SOA  
53 concentration reaches a plateau because of a decrease in precursor concentration), the formed  
54 particles are characterized and a SOA yield is derived. Flow reactors have also been employed  
55 to study SOA formation. <sup>5,6</sup> Such studies improve the understanding of SOA formation under  
56 relatively simple and controllable conditions, but do not completely represent realistic  
57 atmospheric conditions. Limitations of such techniques include limited residence time,  
58 insufficient levels of oxidation, and the wall loss of gas phase compounds and particles. <sup>5,7</sup>

59 Models of SOA formation usually also rely on simplifications. <sup>1</sup> One common simplification is to  
60 ignore individual molecular species and instead use surrogates to represent the complex  
61 mixtures present in aerosol. These models, including the two-product model and the volatility  
62 basis set (VBS) approach, predict SOA mass based on volatility distribution of oxidation  
63 products experimentally derived in chamber studies. <sup>8,9</sup> More recently models have been  
64 developed that take into consideration the molecular identity of the particle-forming  
65 compounds. <sup>10-15</sup> Such models predict SOA formation without relying on experimental SOA  
66 parameterizations. However, computational requirements currently limit the application of  
67 these more explicit approaches and prediction of SOA formation in most operational, large-

68 scale models relies on either the two-product model or VBSs.<sup>16-19</sup> Therefore, the models, too,  
69 may be affected by the limitations of the chamber studies that generated the parameters  
70 calibrating those approaches.

71 Here we will argue that some of the paradigms in SOA-formation-research need to be revisited.  
72 The concept of SOA yield needs to be clarified because the integrative yield that is commonly  
73 determined from chamber experiments (i.e. the mass of SOA produced per mass of reacted  
74 precursor) is different from the differential yield (i.e. the mass of SOA formed upon addition of  
75 oxidation products to an atmosphere already containing such products and SOA) and the latter  
76 is more relevant in the ambient atmosphere. Jiang<sup>20</sup> first introduced such a concept under the  
77 name “instantaneous SOA yield” in 2003. He defined a mathematical expression of this new  
78 concept and applied the two-product form of the equation to calculate SOA yield in chamber  
79 experiments. Here, we try to introduce this concept again using the term “differential yield”  
80 which we find more intuitive. We do not aim to calculate the differential yield using  
81 mathematical formulas as have been introduced and discussed by Jiang,<sup>20</sup> instead our objective  
82 is to raise awareness that the scenarios for which SOA yields have been studied experimentally  
83 so far are not necessarily those that are realistic in an atmospheric context. Most approaches to  
84 obtaining SOA mass in chamber studies do not account for the dynamic nature of SOA  
85 formation, i.e., the process of continuous emission and oxidation of precursor compounds and  
86 its effect on the gas-particle partitioning of the oxidation products and thus the formation of  
87 SOA. In a more realistic scenario, SOA precursors are continuously emitted to the atmosphere,  
88 which usually contains a considerable amount of particles, volatile organic compounds (VOCs),  
89 and semi-volatile organic compounds (SVOCs). There are potentially large uncertainties when  
90 applying SOA parameterization (based on either two-product model or VBS) from unrealistic  
91 experimental scenarios to the ambient atmosphere. In this study, we use a hypothetical  
92 experiment to study a scenario of SOA formation in which precursor is supplied and oxidized  
93 continuously. This is not necessarily more realistic than the scenarios studied in the literature  
94 already but it shows that other scenarios might be possible and that in these other scenarios  
95 SOA formation might follow other rules than those deemed important so far. In addition, with  
96 our modeling approach, we were able to investigate the differential yield for individual SOA

97 forming compounds with different properties and their varying behavior upon changes of the  
98 atmosphere (especially a compositional change of the absorbing phase). Finally, we argue that  
99 SOA formation can only be understood correctly if it is viewed as a result of many competing  
100 kinetic processes.

## 101 **2. Method**

102 Our approach considers a hypothetical scenario involving a parcel of the atmosphere ( $1 \text{ m}^3$ ,  
103 containing a fixed amount of water and ammonium sulfate) that is assumed to receive a  
104 mixture of oxidation products of  $\alpha$ -pinene ozonolysis (of constant composition, details in **Table**  
105 **S1 and Figure S1**), yet experiences neither loss of chemicals and particles nor is being diluted  
106 with clean air. SOA is formed from the equilibrium partitioning of those products between the  
107 gas and the condensed phase, which is assumed to separate into an organic-enriched phase  
108 and an aqueous-electrolyte enriched phase.  $1 \mu\text{g}$  aliquots of the mixture of oxidation products  
109 are added to the atmospheric parcel repeatedly (for a total of 200 times), and are allowed to  
110 achieve equilibrium partitioning after each addition step. The longer this model “experiment”  
111 runs, the more is SOA yield and composition expected to differ from the very beginning of the  
112 experiment. By explicitly considering the molecules involved in SOA formation we can  
113 investigate the SOA yield of individual oxidation products with different volatilities and the yield  
114 change upon addition of more oxidation products. We disregard time in this hypothetical  
115 scenario because we (i) focus on the formation of SOA as a function of the amount of added  
116 oxidation products/precursors and (ii) assume instantaneous equilibrium partitioning between  
117 gaseous and particulate phase.

118 The gas-particle partitioning equilibrium calculations were performed using the commercial  
119 software *COSMOtherm*,<sup>21, 22</sup> as described previously in Wang et al.<sup>10</sup> The focus here is on the  
120 calculated yields, and the procedure used for quantifying gas-particle partitioning is secondary  
121 and therefore only provided in the supplementary information.

## 122 3. Results

### 123 3.1 Definition of SOA Yield

124 The concept of SOA yield is an important parameter in modeling the formation of SOA. SOA  
125 yield ( $Y_{int,p}$ ) is often defined as the amount of SOA formed ( $\Delta M_{SOA}$ ) from certain amount of  
126 precursor reacted ( $\Delta M_p$ ).<sup>8, 23</sup> We call this an **integrative yield** based on reacted precursors ( $Y_{int,p}$ ):

$$127 Y_{int,p} = \Delta M_{SOA} / \Delta M_p \quad (1)$$

128 Another way to define the **integrative yield** ( $Y_{int,op}$ ) is to describe the SOA mass formed ( $\Delta M_{SOA}$ )  
129 from certain amount of oxidation products ( $\Delta M_{op}$ ), i.e. the fraction of oxidation products that  
130 end up making SOA mass:

$$131 Y_{int,op} = \Delta M_{SOA} / \Delta M_{op} \quad (2)$$

132 Because the reaction yield of each oxidation product of  $\alpha$ -pinene was assumed constant in this  
133 study (Table S1) and the ratio between the mass of oxidation products formed ( $\Delta M_{op}$ ) and the  
134 mass of  $\alpha$ -pinene reacted ( $\Delta M_p$ ) is 1.32 (calculated from reaction yield in Table S1),  $Y_{int,op}$  equals  
135 1.32  $Y_{int,p}$  for this study.

136 However, in the atmosphere formation of aerosol is continuous, without an explicit beginning  
137 and end. An integrative yield cannot be a suitable parameter for describing this ongoing aerosol  
138 formation process. What is needed instead is the yield, which describes how much aerosol is  
139 formed in the system upon addition of reaction products at its actual state. Accordingly, we  
140 define the **differential yield** ( $Y_{diff}$ ) as the fraction that partitions to the organic phase ( $dM_{SOA}$ )  
141 when a small amount of oxidation products ( $dM_{op}$ ) is added to the system at a specific loading  
142 of the atmosphere.

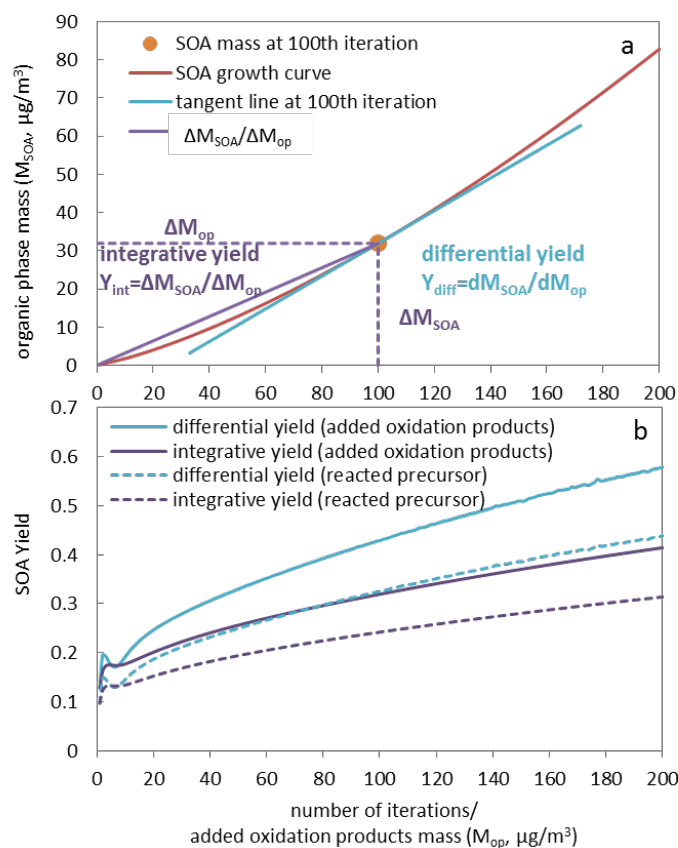
$$143 Y_{diff,op} = dM_{SOA} / dM_{op} \quad (3)$$

144 The differential yield can also be calculated with respect to the reacted amount of precursor,  
145 which is the yield of SOA ( $Y_{diff,p}$ ) after a small amount of precursor has reacted ( $dM_p$ ).

$$146 Y_{diff,p} = dM_{SOA} / dM_p \quad (4)$$

147 The curves showing the growth of the SOA organic phase mass during the iterations of our  
148 hypothetical experiment (Figure 1a) illustrate the difference between integrative and  
149 differential yield. The slope of the purple line in Figure 1a represents the integrative yield. The

150 first derivative of the growth curve (i.e. the tangent of the red line in Figure 1a) represents the  
 151 differential yield at this point of the curve, which is the slope of the blue line in Figure 1a. Figure  
 152 S3 similarly displays the total mass of SOA formed against the reacted amount of precursor. The  
 153 integrative and differential yields based on oxidation products and reacted precursors for our  
 154 hypothetical experiment are plotted in Figure 1b. SOA yields are also plotted against total  
 155 organic phase mass and compared with laboratory generated yields as chamber studies usually  
 156 report SOA yields at different aerosol loadings (Figure S4 and S5). There is a general agreement  
 157 between our prediction and laboratory studies, showing increasing yields with increasing SOA  
 158 loading (Figure S5). Interestingly, because the SOA growth curve is convex, the differential yield  
 159 is always higher than the corresponding integrative yield (see also Jiang<sup>20</sup>). This is because the  
 160 slope of the tangent line at one point is always larger than the slope of the line from this point  
 161 through the origin.



162  
 163 **Figure 1** Organic phase mass (red curve in panel a) and SOA yields (panel b) as a function of the number  
 164 of iterations. The x-axis also represents the total mass of oxidation products added to the

165 system ( $\mu\text{g}/\text{m}^3$ ). In panel a, the orange dot shows the organic phase mass at the 100<sup>th</sup> iteration.  
166 The slope of the blue and purple lines shows the differential and integrative SOA yield,  
167 respectively. In panel b, both integrative yield (purple lines) and differential yield (blue lines) are  
168 calculated without including the aqueous phase. Water as a component in the organic phase is  
169 included. The dashed lines are SOA yields based on the amount of reacted precursor, which  
170 differ from the yields based on added oxidation products (solid lines) by a factor of 1.32.

171 The aqueous phase's contribution to the aerosol loading is quite small and becomes relatively  
172 insignificant as the mass of the organic phase increases for the  $\alpha$ -pinene SOA system (Figure S2).  
173 In the discussion and comparison of SOA yields, the aqueous phase contribution to the overall  
174 SOA yield is therefore not included, i.e., the term SOA yield refers to the yield in the organic  
175 phase, which usually dominates overall SOA growth, especially at higher loadings. However, for  
176 other aerosol systems, the contribution of aqueous phase and multiphase chemistry can be  
177 significant, such as glyoxal SOA, for which aqueous phase chemistry, i.e. reactive uptake other  
178 than equilibrium partitioning, needs to be considered. Note that below we are using the  
179 differential yield based on oxidation products.

180 Similar to the definition of overall differential and integrative yields in equations (1) to (4), we  
181 can define the yield for an individual compound  $i$  based on the added amount of this oxidation  
182 product as follows:

$$183 \quad Y_{diff,i} = dM_{SOA,i} / dM_{op,i} \quad (5)$$

$$184 \quad Y_{int,i} = \Delta M_{SOA,i} / \Delta M_{op,i} \quad (6)$$

185 where  $Y_{diff,i}$  is compound  $i$ 's differential yield, that is the SOA formed ( $dM_{SOA,i}$ ) from a small  
186 amount of added compound  $i$  ( $dM_{op,i}$ ), and  $Y_{int,i}$  is the integrative yield for compound  $i$  defined  
187 as the ratio of SOA formed ( $\Delta M_{SOA,i}$ ) when  $\Delta M_{op,i}$  of compound  $i$  has been added.

### 188 **3.2 Hypothetical SOA Formation Experiment**

189 In the ambient atmosphere SOA is formed constantly with no clearly defined start or end.  
190 Oxidation products are continuously formed in an atmosphere that already contains particles of  
191 various loadings, compositions and sizes (which are quite different from seed particles used in  
192 chamber experiments) and at the same time particles are subject to constant removal by wet or

193 dry deposition, evaporation or condensation due to temperature change, or dilution or  
194 concentration by mixing processes. Thus realistic atmospheric conditions are quite different  
195 from the scenarios that have typically been studied in the lab. The scenario we describe here, in  
196 which oxidation products are constantly added to an atmosphere, is not a realistic scenario  
197 either, because, for example, it ignores particle deposition and disregards the element of time.  
198 Nevertheless, it helps to explore the range of possible scenarios in aerosol formation and how  
199 they may differ from scenarios that have been studied so far.

200 In order to do this, 15  $\alpha$ -pinene oxidation products, which are continuously added to an  
201 atmosphere as described in the Methods section, partition into aerosol particle phase to form  
202 SOA. At equilibrium the mass of compound  $i$  ( $i= 1$  to 15) in the organic phase ( $M_{SOA,i}$ ) can be  
203 described by the following equations when partitioning into an aqueous phase is ignored:

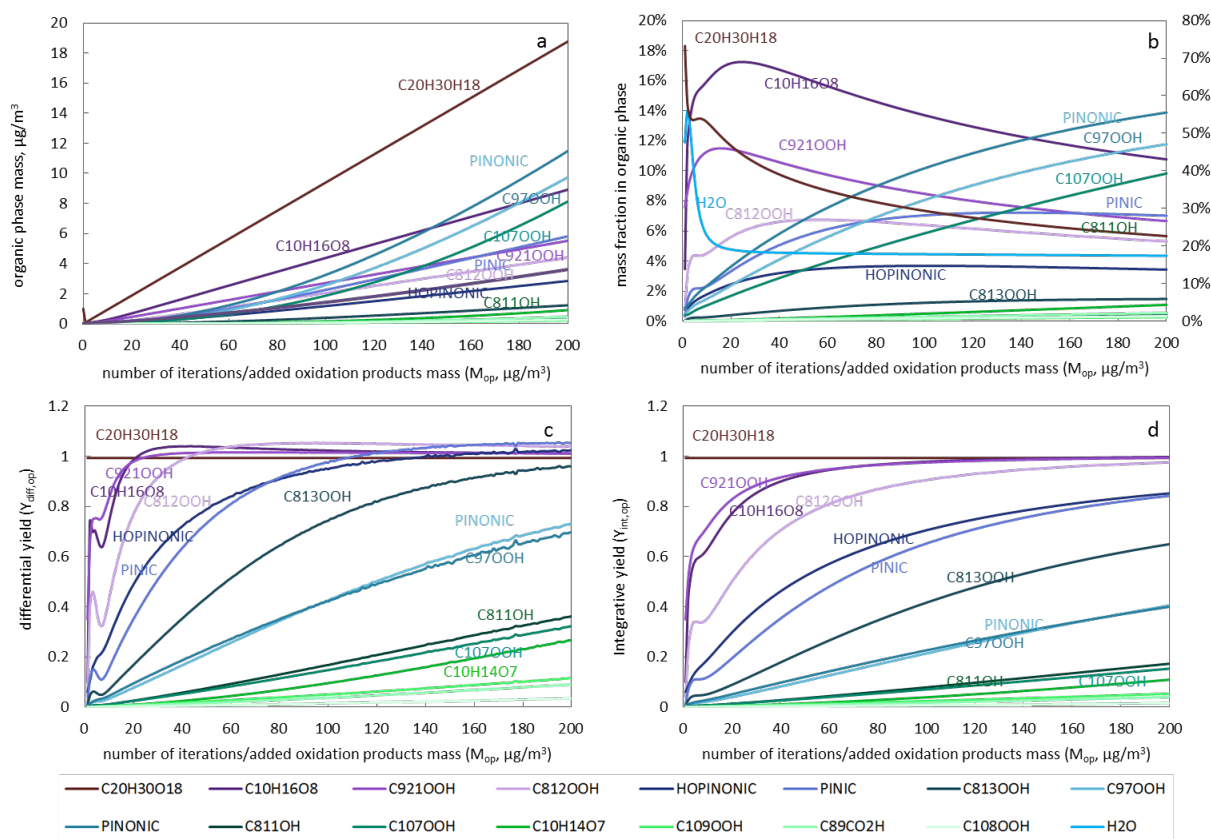
$$204 \quad M_{SOA,i} = M_{op,i} / (1 + 1/(K_{org/gas,i} \cdot M_{SOA}/\rho)) \quad (7)$$

$$205 \quad M_{SOA} = \sum(M_{SOA,i}) \quad (8)$$

206 where  $M_{SOA,i}$  is the amount of compound  $i$  in the organic phase ( $\mu\text{g}/\text{m}^3$ ),  $M_{op,i}$  is the amount of  
207 oxidation product  $i$  in both gas and condensed phase (determined by the reaction yield and the  
208 precursor concentration),  $K_{org/gas,i}$  is the organic-gas phase partition coefficient of compound  $i$   
209 (in unit of  $\text{m}^3 \text{ air} / \text{m}^3 \text{ organic phase}$ ),  $M_{SOA}$  is total organic phase mass in  $\mu\text{g}/\text{m}^3$  and  $\rho$  is the  
210 density of the organic phase ( $\mu\text{g}/\text{m}^3$ ). By calculating the SOA mass formed cumulatively from  
211 the total amount of products added, the integrative SOA can be derived. These equations show  
212 that the SOA yield depends on the partition properties of the reaction products and the  
213 sorptive affinity of the organic phase which both enter into the partition coefficient. In addition,  
214 the yield also depends on the amount of the existing organic mass ( $M_{SOA}$ ), which initially is the  
215 organic seed and later is the sum of all compounds that have partitioned to the organic phase.  
216 For the purpose of our hypothetical experiment, we had to apply equations 7 and 8 iteratively  
217 in small steps because  $K_{org/gas}$  changes in the process due to aerosol composition change and  
218  $M_{SOA}$  depends on the aerosol composition itself. Note, that while the differential yield is given  
219 by the first derivative of equation 7, we cannot evaluate this derivative of  $M_{SOA}$  to  $M_{op}$ , because  
220  $K_{org/gas}$  and  $M_{SOA}$  are complex functions of the actual scenario under consideration. Jiang<sup>20</sup>

221 derived an equation to calculate the instantaneous yield mathematically on the basis of the  
222 Odum two product model without considering the complexity of SOA formation scenarios in  
223 the ambient atmosphere. Knipping et al.<sup>24</sup> commented on the limitation of the equation and  
224 instead recommended a direct partitioning based approach. We agree with Knipping et al.<sup>24</sup>  
225 that neither can a realistic yield be directly calculated from an analytical expression nor can  
226 aerosol formation in an air quality model be simply represented using parameterizations from  
227 unrealistic experimental studies. Instead we have used a direct partitioning based SOA  
228 algorithm as also favored by Knipping et al..<sup>24</sup> Although SOA yield may not be a necessary  
229 parameter in realistic atmosphere and in explicit models, the concept of a differential yield is  
230 useful to analyze and compare various scenarios and oxidation products in their efficiency to  
231 produce secondary aerosols.

232 To study the contribution of an individual oxidation product to the growth of SOA and the  
233 influencing factors, the growth curve of individual compounds, the SOA composition and the  
234 individual SOA yield are plotted in Figure 2. Generally, both the differential and integrative SOA  
235 yields increase with increasing number of iterations (Figure 2c and 2d). The differential yield for  
236 each component is always higher than the integrative yield, except for C<sub>20</sub>H<sub>30</sub>O<sub>18</sub>, and the  
237 difference is larger for more volatile compounds (See Figure S6). There are some fluctuations in  
238 the first few iterations, which are due to the initially rapid compositional change (as shown in  
239 Figure 2b). During the first few iterations the change of phase composition depends on the  
240 composition and mass of the organic seed assumed to be present initially (see SI). However,  
241 these initial conditions quickly lose their influence on the partitioning properties when the SOA  
242 mass increases.



243

244 **Figure 2** Organic phase mass (panel a), composition (panel b), differential and integrative yields (panel c  
 245 and d) as a function of the added oxidation products (same as number of iterations). In panel b,  
 246 the mass fraction of  $\text{C}_{20}\text{H}_{30}\text{O}_{18}$  is shown on the right y-axis. Major contributors to the particles  
 247 are labeled with their names.

248  $\text{C}_{20}\text{H}_{30}\text{O}_{18}$ , an extremely low volatile compound (ELVOC), has a differential yield of 1 at  
 249 different SOA loadings (the dark red line in **Figure 2c**). Similarly, the integrative yield is also 1  
 250 (**Figure 2d**). This is reasonable because as long as it is formed it will prefer the condensed phase  
 251 due to its extremely low volatility. The partitioning behaviour of such ELVOCs is largely  
 252 independent of vapor pressures or partitioning coefficients and existing particle mass and  
 253 composition. Thus, the difference between their differential and integrative yield is small. Even  
 254 though  $\text{C}_{20}\text{H}_{30}\text{O}_{18}$  has a very low reaction yield (molar yield in **Table S1**), it is still the  
 255 dominant component in the organic phase due to its high  $K_{org/gas}$  (**Figure S7**). Its contribution is  
 256 decreasing as more SVOC compounds with lower  $K_{org/gas}$  start to partition into the condensed  
 257 organic phase at higher organic phase loadings (**Figure 2b**). These SVOC such as  $\text{C}_{107}\text{OOH}$ , PINONIC and

258 C97OOH have relatively high reaction yields (molar yield of 0.2385, 0.140 and 0.115 in Table S1).  
259 The mass fraction of these three compounds in the particulate phase is increasing from the first  
260 to the last iteration (Figure 2b).

261 Some compounds, such as C10H16O8, C921OOH, C812OOH, and after the 100<sup>th</sup> iteration also  
262 HOPINONIC and PINIC, have differential yields exceeding 1, i.e., the amount of a compound that  
263 partitions to the organic phase is higher than the amount added in that iteration. The “excess”  
264 amount is compound from previous iterations that had been stored in the gas phase but that  
265 now partitions into the particle phase in addition to the amount just added. Reasons for  
266 differential yields above 1 are the increasing loading of the organic phase and a changing  
267 organic phase composition that becomes more favorable for some of the compounds. For  
268 instance, there is an increase in  $K_{org/gas}$  (and a decrease in activity coefficient) for C10H16O8,  
269 C812OOH and PINIC with more iterations (Figure S7 and S8), indicating that the particle phase  
270 composition becomes more favourable for their solvation. Obviously, the differential yield of  
271 any compound that transitorily exceeds unity has to drop back to unity eventually at higher  
272 loadings. The integrative yield can never exceed 1 (Figure 2d).

273 Once a compound starts to build up higher and higher gas phase concentrations, more of any  
274 additionally added amount of this compound will sorb to the condensed phase no matter its  
275 volatility. The volatility of a compound only determines when it reaches a differential yield of 1,  
276 with less volatile compound reaching that threshold earlier. For example, in Figure 2c the  
277 ELVOC C20H30H18 reaches a differential yield of 1 immediately after it starts to form particles  
278 and the differential yield for other relatively low volatility compounds such as C10H16O8,  
279 C921OOH, C812OOH (with  $\log K_{org/gas}$  higher than 11 in Figure S7) increases quickly to 1 and  
280 above. Eventually, when enough gas phase species have accumulated and when the SOA  
281 loading is high, even relatively volatile compounds will approach a very high differential yield.  
282 While this may seem counter-intuitive at first, it becomes clearer if one realizes that any single  
283 compound continuously added to a finite gas phase will eventually approach its saturation  
284 vapor pressure and from that point onwards any additionally added amount would condense  
285 into its own liquid pure phase i.e. have a differential yield of unity, no matter how volatile it is

286 and no matter how much particulate phase is available. Because SOA formation involves  
287 organic mixtures, eventually not a pure phase of a single chemical is formed but an azeotropic  
288 mixture. The “saturated” gas phase concentrations at which every newly formed product  
289 immediately and completely “condenses” into the azeotrope are typically much smaller than  
290 the saturation vapor concentrations of all the single components themselves. Compounds with  
291  $K_{org/gas}$  (or vapor pressures) differing by orders of magnitude will eventually have similar  
292 differential yields if the particulate phase comes close to an azeotropic mixture. For example,  
293 C<sub>20</sub>H<sub>30</sub>O<sub>18</sub>, C<sub>10</sub>H<sub>16</sub>O<sub>8</sub>, C<sub>9</sub>H<sub>16</sub>O<sub>8</sub>, C<sub>8</sub>H<sub>12</sub>O<sub>8</sub>, HOPINONIC, PINIC and C<sub>8</sub>H<sub>12</sub>O<sub>8</sub> all have  
294 differential yields around 1 at the 200<sup>th</sup> iteration, even though their  $K_{org/gas}$  varies from 10<sup>10</sup> to  
295 10<sup>19</sup> (Figure S7). If we had continued our calculations in Figure 2 much further then eventually  
296 all oxidation products, even the most volatile ones, would have reached a differential yield of  
297 unity and the particulate phase would have become an azeotrope mixture whose composition  
298 would not change any more when more oxidation products (of constant composition) were  
299 added. In this situation the growth of the particle phase would be identical to the addition of  
300 oxidation products so that compounds with highest reaction yields would also dominate  
301 aerosol formation. This agrees with the statement from Seinfeld and Pankow<sup>25</sup> that “the SOA  
302 yield approaches a constant value as the amount of particulate organic into which the gaseous  
303 products absorb reaches large values, and this asymptotic amount is determined purely by  
304 reaction stoichiometry”. Apart from the widely known aerosol loading effect as proposed by  
305 Seinfeld and Pankow,<sup>25</sup> we were also able to demonstrate the effect of changing composition  
306 (i.e. the activity of organic products in the condensed phase) and gas phase accumulation on  
307 SOA formation.

#### 308 **4. Discussion**

309 A realistic scenario of SOA formation has to consider that usually different levels of oxidation  
310 products have accumulated in the gas phase, precursors are emitted constantly and new  
311 oxidation products are formed continuously. Figure 2 illustrates that neither the yield nor the  
312 composition of gas and particle phase at higher loadings can be easily extrapolated from those  
313 measured at lower loadings or vice versa. The formed SOA mass will be higher than traditionally

314 calculated based on chamber experiment fits (either using the two product model or the VBS  
315 approach) by using the differential yield, when considering the continuous emission of  
316 precursors and their oxidation products in the atmosphere.

317 Conventional chamber experiments aid in understanding reaction pathways and kinetics but  
318 they are not providing the SOA formation parameters most relevant to the situation in the real  
319 atmosphere. That situation is dynamic, i.e., varies temporally and spatially with different  
320 loadings of particles and gas phase compounds. When oxidized compounds are formed in a  
321 clean atmosphere without many pre-existing particles, low volatility compounds will partition  
322 to the condensed phase first and the formed particles consist of compounds with low volatility.  
323 Relatively volatile products will remain in the gas phase. In this situation the differential SOA  
324 yield for individual products depends strongly on their partition coefficient and the  
325 concentration of already available sorbing particles. The total yield (i.e. integrated over all  
326 reaction products) depends on the individual yields weighted by the mole fraction that they  
327 contribute to the sum of all reaction products. Thus, quite different total yields are to be  
328 expected for different types and amounts of seed particles but also for different reaction  
329 pathways that may lead to various species and amounts of oxidation products.

330 While the particle grows, more volatile compounds start to partition and contribute to SOA and  
331 thus the SOA yield for individual compounds increases (Figure 2c). This is similar to oxidation  
332 products being emitted to an atmosphere with some pre-existing particles. For example,  
333 partitioning of the compounds to the particles at the 80<sup>th</sup> iteration is very different from  
334 partitioning into the initial particle, because of the different mass (24  $\mu\text{g}$  vs. 0.5  $\mu\text{g}$ ) and  
335 composition (Figure 2a and 2b) of the organic phase. In the extreme, the scenario eventually  
336 converges towards a situation where all oxidation products have a differential yield of unity  
337 independent of their volatility and independent of the amount of available sorbing phase. In  
338 this final state the composition of the particle approaches that of an azeotrope mixture and the  
339 products with the highest reaction yields govern particle growth.

340 In general, we can conclude that close to the source of precursors and with a stable  
341 atmosphere (limited mixing and removal), e.g. a smog situation, the atmosphere is likely to

342 build up substantial gas phase concentrations of partitioning species and thus achieve rather  
343 high yields. The type and amount of existing SOA then has diminished influence on the yield  
344 and even the volatility of the reaction products will become less important. If the atmosphere is  
345 rather clean, well mixed and further away from the emission of precursors, the SOA formation  
346 might be closer to that in the chamber experiments. In summary we conclude that there might  
347 exist scenarios in the atmosphere in which the differential SOA yield is not as dependent on  
348 compound volatility and existing particle mass as has been indicated by chamber experiments  
349 and theoretical investigations previously.

## 350 **5. Looking forward**

351 **Figure 2** illustrates how much the equilibrium partitioning of oxidation products between gas  
352 and particle phase can change if more and more oxidation products are added. The curves in  
353 **Figure 2** change somewhat for different temperatures, relative humidity and/or with different  
354 precursors/oxidation products. However, all of these curves still do not resemble the situation  
355 in the real atmosphere, because the dimension of time is ignored in our “experiment”. The  
356 concentration of gaseous organic compounds depends on their emission or formation rate in  
357 the air compared to the removal rate by sorption, mixing, reaction or deposition. Similarly,  
358 while particles are formed and grow, they are - at the same time - removed from an air parcel  
359 by gravitational settling or washing out or they are exchanged with neighboring air parcels by  
360 turbulent mixing. A realistic treatment cannot separate these processes from the formation of  
361 particles because the amount of existing particles has an immediate feedback on the formation  
362 of new particles. In order to understand aerosol formation in the atmosphere in qualitative and  
363 quantitative terms, it will therefore be necessary to consider the kinetics of many relevant  
364 processes even if one finds that the partition process itself is so quick that it can still be treated  
365 as an instantaneous equilibrium. If an air parcel can be considered stable for a while, a steady-  
366 state situation may arise for which a differential yield could then be calculated. It might be  
367 quite challenging though to establish where this steady-state is located, because it requires  
368 knowledge of the emission rate of precursor gases and primary particles, the reaction rate  
369 constants for all relevant reactions of the precursors, as well as the rate constants for

370 atmospheric mixing, dry and wet deposition, and particle coagulation. Such an analysis will have  
371 to consider the simultaneous existence of particles of differing size and composition, which also  
372 differ in their growth and elimination.

373 Due to the non-linear nature of many of the involved processes, rather small changes in the  
374 boundary conditions may lead to different, stable steady-state situations. Note that SOA  
375 parameterization based on single or a few chamber experiments (i.e. using the volatility  
376 distribution obtained from chamber experiments in the treatment of SOA formation in most  
377 current atmospheric models, e.g. the two-product or VBS approach) may not describe SOA  
378 growth in such a kinetically controlled system in a meaningful way. Such kinetically controlled  
379 systems are far from the thermodynamic considerations that dominate the discussion of  
380 aerosol formation in the literature. We believe research on SOA formation needs to focus on  
381 these kinetic questions and problems. It will be an interesting but also highly demanding task to  
382 unravel the factors that dominate aerosol formation in the real atmosphere. For example,  
383 recent studies have investigated the sensitivity of SOA evolution to different processes and  
384 parameterizations, including emissions, removal processes (such as dry deposition, photolysis  
385 and heterogeneous chemistry) and particle-phase transformation of SOA to low volatility, which  
386 demonstrate that SOA is a far more dynamic system and a subset of complex and uncertain  
387 processes are governing the lifecycle of SOA. <sup>26-28</sup> The ultimate goal is to identify mechanisms  
388 and processes that could be most influential in affecting evolution of SOA and to understand  
389 how different parameters contribute to the overall uncertainty.

390 It is unrealistic to assume the composition and volatility distribution of the oxidation products  
391 in the chamber experiments is the same as in the ambient atmosphere for a specific precursor.  
392 Instead, a direct and explicit prediction of SOA formation is required <sup>24</sup>. Nevertheless, there is  
393 still a use for the SOA yield as a quantitative measure in comparing the efficiency of aerosol  
394 formation under different scenarios for different precursors. In this context it is certainly  
395 important to acknowledge that the differential yield is preferable over the integrative yield.

## 396 Acknowledgement

397 We acknowledge financial support from the Natural Sciences and Engineering Research Council  
398 of Canada, an Ontario Graduate Scholarship and a Special Opportunity Travel Fellowship from  
399 Department of Chemistry at University of Toronto. We thank Arthur Chan and Jon Abbatt for  
400 comments on our manuscript. C.W. is grateful for Stephen Wood's help with coding.

## 401 Electronic Supplementary Information

402 Additional information on the description of method, information for the organic compounds,  
403 aqueous phase composition, comparison with laboratory studies, contribution of water in the  
404 organic phase, comparison with previous studies, and additional tables and figures referenced  
405 in the text is provided in Electronic Supplementary Information.

## 406 References

- 407 1. M. Hallquist, J. C. Wenger, U. Baltensperger, Y. Rudich, D. Simpson, M. Claeys, J. Dommen, N. M.  
408 Donahue, C. George, A. H. Goldstein, J. F. Hamilton, H. Herrmann, T. Hoffmann, Y. Iinuma, M.  
409 Jang, M. E. Jenkin, J. L. Jimenez, A. Kiendler-Scharr, W. Maenhaut, G. McFiggans, T. F. Mentel, A.  
410 Monod, A. S. H. Prevot, J. H. Seinfeld, J. D. Surratt, R. Szmigielski and J. Wildt, *Atmospheric  
411 Chemistry and Physics*, 2009, **9**, 5155-5236.
- 412 2. M. Glasius and A. H. Goldstein, *Environmental Science & Technology*, 2016, **50**, 2754-2764.
- 413 3. E. A. Brunns, I. El Haddad, A. Keller, F. Klein, N. K. Kumar, S. M. Pieber, J. C. Corbin, J. G. Slowik, W.  
414 H. Brune, U. Baltensperger and A. S. H. Prévôt, *Atmos. Meas. Tech.*, 2015, **8**, 2315-2332.
- 415 4. J. E. Shilling, Q. Chen, S. M. King, T. Rosenoern, J. H. Kroll, D. R. Worsnop, K. A. McKinney and S. T.  
416 Martin, *Atmos. Chem. Phys.*, 2008, **8**, 2073-2088.
- 417 5. A. T. Lambe, P. S. Chhabra, T. B. Onasch, W. H. Brune, J. F. Hunter, J. H. Kroll, M. J. Cummings, J.  
418 F. Brogan, Y. Parmar, D. R. Worsnop, C. E. Kolb and P. Davidovits, *Atmos. Chem. Phys.*, 2015, **15**,  
419 3063-3075.
- 420 6. A. T. Lambe, A. T. Ahern, L. R. Williams, J. G. Slowik, J. P. S. Wong, J. P. D. Abbatt, W. H. Brune, N.  
421 L. Ng, J. P. Wright, D. R. Croasdale, D. R. Worsnop, P. Davidovits and T. B. Onasch, *Atmos. Meas.  
422 Tech.*, 2011, **4**, 445-461.
- 423 7. X. Zhang, C. D. Cappa, S. H. Jathar, R. C. McVay, J. J. Ensberg, M. J. Kleeman and J. H. Seinfeld,  
424 *Proceedings of the National Academy of Sciences of the United States of America*, 2014, **111**,  
425 5802-5807.
- 426 8. J. R. Odum, T. Hoffmann, F. Bowman, D. Collins, R. C. Flagan and J. H. Seinfeld, *Environ. Sci.  
427 Technol.*, 1996, **30**, 2580-2585.
- 428 9. N. M. Donahue, A. L. Robinson, C. O. Stanier and S. N. Pandis, *Environmental Science &  
429 Technology*, 2006, **40**, 2635-2643.
- 430 10. C. Wang, K.-U. Goss, Y. D. Lei, J. P. D. Abbatt and F. Wania, *Environmental Science & Technology*,  
431 2015, **49**, 8585-8594.
- 432 11. A. Zuend and J. H. Seinfeld, *Atmospheric Chemistry and Physics*, 2012, **12**, 3857-3882.

- 433 12. J. Li, M. Cleveland, L. D. Ziemba, R. J. Griffin, K. C. Barsanti, J. F. Pankow and Q. Ying, *Atmospheric*  
434 *Environment*, 2015, **102**, 52-61.
- 435 13. J. F. Pankow, M. C. Marks, K. C. Barsanti, A. Mahmud, W. E. Asher, J. Li, Q. Ying, S. H. Jathar and  
436 M. J. Kleeman, *Atmospheric Environment*, 2015, **122**, 400-408.
- 437 14. B. Aumont, R. Valorso, C. Mouchel-Vallon, M. Camredon, J. Lee-Taylor and S. Madronich, *Atmos.*  
438 *Chem. Phys.*, 2012, **12**, 7577-7589.
- 439 15. J. Lee-Taylor, S. Madronich, B. Aumont, A. Baker, M. Camredon, A. Hodzic, G. S. Tyndall, E. Apel  
440 and R. A. Zaveri, *Atmos. Chem. Phys.*, 2011, **11**, 13219-13241.
- 441 16. A. G. Carlton, P. V. Bhave, S. L. Napelenok, E. O. Edney, G. Sarwar, R. W. Pinder, G. A. Pouliot and  
442 M. Houyoux, *Environmental Science & Technology*, 2010, **44**, 8553-8560.
- 443 17. H. O. T. Pye, A. W. H. Chan, M. P. Barkley and J. H. Seinfeld, *Atmos. Chem. Phys.*, 2010, **10**,  
444 11261-11276.
- 445 18. S. C. Farina, P. J. Adams and S. N. Pandis, *Journal of Geophysical Research-Atmospheres*, 2010,  
446 **115**.
- 447 19. K. Tsigaridis, N. Daskalakis, M. Kanakidou, P. J. Adams, P. Artaxo, R. Bahadur, Y. Balkanski, S. E.  
448 Bauer, N. Bellouin, A. Benedetti, T. Bergman, T. K. Berntsen, J. P. Beukes, H. Bian, K. S. Carslaw,  
449 M. Chin, G. Curci, T. Diehl, R. C. Easter, S. J. Ghan, S. L. Gong, A. Hodzic, C. R. Hoyle, T. Iversen, S.  
450 Jathar, J. L. Jimenez, J. W. Kaiser, A. Kirkevåg, D. Koch, H. Kokkola, Y. H. Lee, G. Lin, X. Liu, G. Luo,  
451 X. Ma, G. W. Mann, N. Mihalopoulos, J. J. Morcrette, J. F. Müller, G. Myhre, S. Myriokefalitakis, N.  
452 L. Ng, D. O'Donnell, J. E. Penner, L. Pozzoli, K. J. Pringle, L. M. Russell, M. Schulz, J. Sciare, Ø.  
453 Seland, D. T. Shindell, S. Sillman, R. B. Skeie, D. Spracklen, T. Stavrakou, S. D. Steenrod, T.  
454 Takemura, P. Tiitta, S. Tilmes, H. Tost, T. van Noije, P. G. van Zyl, K. von Salzen, F. Yu, Z. Wang, R.  
455 A. Zaveri, H. Zhang, K. Zhang, Q. Zhang and X. Zhang, *Atmos. Chem. Phys.*, 2014, **14**, 10845-  
456 10895.
- 457 20. W. Jiang, *Atmospheric Environment*, 2003, **37**, 5439-5444.
- 458 21. A. Klamt and F. Eckert, *Fluid Phase Equilibria*, 2000, **172**, 43-72.
- 459 22. A. Klamt, *From Quantum Chemistry to Fluid Phase Thermodynamics and Drug Design*, Elsevier,  
460 Amsterdam, 2005.
- 461 23. J. F. Pankow, *Atmospheric Environment*, 1994, **28**, 189-193.
- 462 24. E. M. Knipping, R. J. Griffin, F. M. Bowman, B. Pun, C. Seigneur, D. Dabdub and J. H. Seinfeld,  
463 *Atmospheric Environment*, 2004, **38**, 2759-2761.
- 464 25. J. H. Seinfeld and J. F. Pankow, *Annual Review of Physical Chemistry*, 2003, **54**, 121-140.
- 465 26. M. Shrivastava, C. Zhao, R. C. Easter, Y. Qian, A. Zelenyuk, J. D. Fast, Y. Liu, Q. Zhang and A.  
466 Guenther, *Journal of Advances in Modeling Earth Systems*, 2016, **8**, 499-519.
- 467 27. A. Hodzic, P. S. Kasibhatla, D. S. Jo, C. D. Cappa, J. L. Jimenez, S. Madronich and R. J. Park, *Atmos.*  
468 *Chem. Phys.*, 2016, **16**, 7917-7941.
- 469 28. K. Tsigaridis, N. Daskalakis, M. Kanakidou, P. J. Adams, P. Artaxo, R. Bahadur, Y. Balkanski, S. E.  
470 Bauer, N. Bellouin, A. Benedetti, T. Bergman, T. K. Berntsen, J. P. Beukes, H. Bian, K. S. Carslaw,  
471 M. Chin, G. Curci, T. Diehl, R. C. Easter, S. J. Ghan, S. L. Gong, A. Hodzic, C. R. Hoyle, T. Iversen, S.  
472 Jathar, J. L. Jimenez, J. W. Kaiser, A. Kirkevåg, D. Koch, H. Kokkola, Y. H. Lee, G. Lin, X. Liu, G. Luo,  
473 X. Ma, G. W. Mann, N. Mihalopoulos, J. J. Morcrette, J. F. Müller, G. Myhre, S. Myriokefalitakis, N.  
474 L. Ng, D. O'Donnell, J. E. Penner, L. Pozzoli, K. J. Pringle, L. M. Russell, M. Schulz, J. Sciare, Ø.  
475 Seland, D. T. Shindell, S. Sillman, R. B. Skeie, D. Spracklen, T. Stavrakou, S. D. Steenrod, T.  
476 Takemura, P. Tiitta, S. Tilmes, H. Tost, T. van Noije, P. G. van Zyl, K. von Salzen, F. Yu, Z. Wang, R.  
477 A. Zaveri, H. Zhang, K. Zhang, Q. Zhang and X. Zhang, *Atmospheric Chemistry and Physics*, 2014,  
478 **14**, 10845-10895.

479